Journal of Magnetic Resonance 242 (2014) 57–66

Contents lists available at ScienceDirect

Journal of Magnetic Resonance

journal homepage: www.elsevier.com/locate/jmr

General expressions for the coupling coefficient, quality and filling factors for a cavity with an insert using energy coupled mode theory

Sameh Y. Elnaggar [a], Richard Tervo [a], Saba M. Mattar [b,*]

[a] Department of Electrical and Computer Engineering, University of New Brunswick, Fredericton, New Brunswick E3B 6E2, Canada
[b] Department of Chemistry and Centre for Laser, Atomic and Molecular Sciences, University of New Brunswick, Fredericton, New Brunswick E3B 6E2, Canada

ARTICLE INFO

Article history:
Received 6 September 2013
Revised 27 January 2014
Available online 14 February 2014

Keywords:
Electron paramagnetic resonance
Dielectric resonators
Resonance cavity
Resonator modes
Coupled mode theory
Coupled modes
Coupling coefficient
Quality factor
Filling factor
Resonator frequency
Finite element methods
Magnetic field distributions
Electric field distributions
Spectrometer sensitivity
Signal-to-noise ratio

ABSTRACT

A cavity (CV) with a dielectric resonator (DR) insert forms an excellent probe for the use in electron paramagnetic resonance (EPR) spectrometers. The probe's coupling coefficient, κ, the quality factor, Q, and the filling factor, η are vital in assessing the EPR spectrometer's performance. Coupled mode theory (CMT) is used to derive general expressions for these parameters. For large permittivity the dominating factor in κ is the ratio of the DR and CV cross sectional areas rather than the dielectric constant. Thus in some cases, resonators with low dielectric constant can couple much stronger with the cavity than do resonators with a high dielectric constant. When the DR and CV frequencies are degenerate, the coupled η is the average of the two uncoupled ones. In practical EPR probes the coupled η is approximately half of that of the DR. The Q of the coupled system generally depends on the eigenvectors, uncoupled frequencies (ω_1, ω_2) and the individual quality factors (Q_1, Q_2). It is calculated for different probe configurations and found to agree with the corresponding HFSS® simulations. Provided there is a large difference between the Q_1, Q_2 pair and the frequencies of DR and CV are degenerate, Q is approximately equal to double the minimum of Q_1 and Q_2. In general, the signal enhancement ratio, $I_{with\ insert}/I_{empty}$, is obtained from Q and η. For low loss DRs it only depends on η_1/η_2. However, when the DR has a low Q, the uncoupled Qs are also needed. In EPR spectroscopy it is desirable to excite only a single mode. The separation between the modes, Φ, is calculated as a function of κ and Q. It is found to be significantly greater than five times the average bandwidth. Thus for practical probes, it is possible to excite one of the coupled modes without exciting the other. The CMT expressions derived in this article are quite general and are in excellent agreement with the lumped circuit approach and finite numerical simulations. Hence they can also be applied to a loop-gap resonator in a cavity. For the design effective EPR probes, one needs to consider the κ, Q and η parameters.

1. Introduction

A large number of biological molecules of medicinal significance contain unpaired electrons and are paramagnetic. As a result comprehending their magneto-structural properties, such as geometry, electronic structure–function relationships, spin–spin distances and gyromagnetic, fine, and hyperfine tensors is of crucial importance. Pulsed or continuous-wave (CW) electron resonance techniques, such as electron paramagnetic resonance (EPR) [1,2], electron–nuclear double resonance (ENDOR) [3,4], electron–electron double resonance (ELDOR) [5,6], electron spin echo envelope modulation (ESEEM) [7,8], double quantum coherence (DQC) [9–11] and pulsed ELDOR, also known as DEER [7,12–14], are powerful spectroscopic methods for studying the properties of paramagnetic molecules.

Usually these biological molecules are large and the number of paramagnetic moieties in comparison to the overall molecule is small. Thus they are considered to be paramagnetically dilute. In addition, the sample size is generally small and its quantity is limited. Consequently, in the past few years extensive research and effort is spent on increasing the sensitivity of the spectrometers. A major thrust in this domain is to design probes that are more sensitive. Accordingly, miniature loop-gap (LGR) [15–17] or dielectric (DR) [18–25] resonators were introduced as probe components. These resonators have small sizes, high energy density and large magnetic fields ($\mathbf{B_1}$) in the sample vicinity (filling factors) [16–22,24–27].

Loop gap resonators and DRs are normally housed in a shield to confine the probe's microwave radiation. Cavities may be

* Corresponding author. Fax: +1 506 453 4981.
E-mail address: mattar@unb.ca (S.M. Mattar).

http://dx.doi.org/10.1016/j.jmr.2014.01.018
1090-7807/

considered as large microwave shields and have also been used to house LGRs and DRs [28]. Different groups have used a *single* resonator placed in a cavity [18,19,23–27]. A similar probe was employed in our laboratory that consists of *two* dielectric resonators ($\varepsilon_r = 29.2$), asymmetrically placed in a rectangular TE_{102} cavity. The resulting DR/TE_{102} probe has a signal to-noise-ratio (SNR) is at least 24 times larger than the conventional TE_{102} cavity alone [21].

Most of the work performed has mainly been empirical in nature. With the advent of sophisticated electron magnetic resonance techniques, the majority of researchers have become familiar with the probe's performance parameters, such as quality factors, Q and filling factors, η. They are now routinely taken into consideration when designing complex experiments. Therefore it is essential that, starting from first principles, one understands theoretically the coupling between the different components such as the cavity, DRs or LGRs, in order to optimize efficient magnetic resonance probes. A particularly useful endeavor is to derive analytical expressions, in closed form, that give insight and predict the frequencies, electromagnetic field distributions, η, Q of the probe's modes and coupling constants, κ, between its resonating components. The accuracy of the predicted frequency modes and electromagnetic field distributions are then compared with numerical finite element simulations.

For example, the frequency-field distributions and filling factors of the DR/TE_{102} probe were simulated and analyzed by finite element methods [29]. It was shown that the three resonating modes couple to form three coupled modes. The resonant cavity was determined to be an essential component of the probe that affects its frequency.

Theoretical treatment of magnetic resonance probes is rare. In a seminal paper, Mett et al. were among the first to simulate the effect of a cylindrical cavity as a resonating entity on a single dielectric resonator. The results were compared with an equivalent circuit model [30]. In a parallel fashion the current authors, starting from first principles and Maxwell's equations, developed a coupled mode theory in the form of an eigenvalue problem [31]. It was used to analyze the properties of a probe consisting of a DR inserted in a cavity. By solving the eigenvalue problem, the predominant coupled modes (symmetric and anti-symmetric) were found. The frequencies and fields were also calculated. As the next logical step, in this article equations and expressions for the filling factor, quality factor and coupling coefficients, which are important in understanding the behavior of EPR probes, are derived.

As previously mentioned, a probe consisting of a loop-gap (LGR) or a dielectric resonator (DR) inserted in a conducting cavity (CV) significantly enhances the signal-to-noise ratio (SNR) of its electron paramagnetic resonance (EPR) spectrometer [18,19,21,22]. For a certain resonance frequency, f, the size of a DR or a LGR is much smaller than that of a CV. Accordingly, the filling factor of the probe increases due to the compactness of the magnetic fields inside and in the vicinity of the inserted resonator [22]. When the frequencies of the DR $TE_{01\delta}$ mode and that of the rectangular CV TE_{102} mode (or cylindrical CV TE_{011} mode) are close (near degenerate), the energy exchange between the two modes is a maximum [31]. This situation, is helpful if, in designing an experiment, one needs to enhance the signal intensity of a standard conventional CV without modifying the coupling to the microwave bridge [22]. However if signal enhancement is of a higher priority, a DR material inserted in a shield would have a better SNR [18,30]. In the latter case, the coupling to the microwave bridge through an iris on the shield surface may be unachievable [30]. Two dielectric resonators inserted in a cavity give the user the ability and flexibility to tune the frequency of the probe in addition to improving the SNR [21,29,32].

The electromagnetic interactions among the individual components of an EPR probe are of vital importance. The coupling between the $TE_{01\delta}$ DR mode and the TE_{011} cylindrical CV mode was studied in Ref. [30] using a lumped circuit model (LCM) and in Ref. [31] using coupled mode theory (CMT). The LCM was used to calculate different probe parameters, such as coupled frequencies, quality factors and resonator efficiencies. The interaction of both modes results in two coupled ones: a symmetric (parallel) mode and an anti-symmetric (anti-parallel) mode [31]. CMT, when applied, was able to determine the coupled fields in addition to the frequencies. This suggests that the coupling coefficient, κ, quality factor, Q and filling factor, η can also be studied using CMT. The analytical equations derived here using CMT give new insight for κ, Q and η.

The coupling coefficient, κ, between two resonators, such as the DR and CV, is a measure of how strong they couple. This parameter, as used in the current article, is not to be confused with the coupling coefficient used to study how efficient a particular microwave mode of the probe is coupled to the spectrometer's microwave bridge. For DRs with moderate relative dielectric constants ($\varepsilon_r \approx 20 - 50$) the coupling coefficient between the CV and DR modes is significantly high, particularly when the cavity's dimensions shrink [31]. Thus the modes are still coupled even though the frequency difference between them is large [31]. The significant presence of the DR mode, reflected by a large κ value, influences the probe filling factor and hence the signal intensity. In contrast, for high dielectric constants ($\varepsilon_r \approx 100 - 300$) κ decreases and the modes tend to decouple [30]. Therefore it is important to understand how the coupling coefficient depends on the permittivity and the geometric dimensions. One of the aims of the current paper is to answer this question.

Moreover, the coupling coefficient is also crucial in determining whether or not exciting one coupled mode will excite the other. To excite a particular mode, the driving source's frequency should be within $\pm 5BW = \pm 5(f/Q)$ of the mode's frequency [30]. Here BW is the mode bandwidth. Consequently, to avoid exciting other spurious modes their frequencies should be at least five times the bandwidth away from the desired mode. Therefore the frequency separation of the two coupled modes and the average bandwidth (BW_{avg}) of the two modes need to be understood.

The bandwidth is inversely proportional to the quality factor [33]. Depending on the frequency difference between the two uncoupled modes, the quality factor changes tremendously [30]. Consequently, it is crucial that one is able to predict beforehand the Q behavior of the coupled system.

The intensity of an EPR signal depends on numerous factors. Some of these factors are characteristic of the paramagnetic sample while others depend on the spectrometer and its probe. Detailed reviews of this subject have been undertaken [34–36]. The signal voltage, V_S at the interface between the spectrometer's microwave bridge and the probe is directly proportional to the signal intensity. It is

$$V_S = \chi'' \eta Q \sqrt{PZ_0},$$

where Z_0 is the characteristic impedance of the microwave bridge and P is the incident microwave power coupled to the probe. The magnetic susceptibility of the sample, χ'', is the imaginary component of the magnetic susceptibility. Thus, for unsaturated samples, the signal intensity, I, for EPR probes is proportional to the resonator's parameters [22,37,38]

$$I \propto \eta Q \sqrt{P}. \tag{1}$$

Although a dielectric insert or a loop-gap may increase the filling factor, the quality factor may decrease in such a way that the enhancement in the signal intensity may be affected [22,30]. How the filling factor changes with coupling is another important question that needs to be answered.

For the above reasons, the aim of this paper is to derive analytical expressions for the coupling coefficient, quality factor and the filling factor of a system consisting of a dielectric resonator inserted in a cavity. This is achieved using CMT. It is also assumed that the findings here can be directly applied to the case of a loop-gap resonator inserted in a cavity.

Section 2 concisely defines the coupled system where previously derived properties using CMT such as the frequencies, eigenvectors and the electric fields were presented. Using CMT, expressions for the coupling coefficient, the quality and the filling factors are derived in Section 3. This section forms the main core needed to study the system at hand. In addition, results and discussion of these parameters are also included as subsections. Coupling coefficients, filling factors and quality factors are discussed in Sections 3.1-3.3 respectively. The results are verified using finite element simulations. Finally, a summary and conclusions are provided in Section 4.

2. Theoretical background

The system under consideration is depicted in Fig. 1. It consists of a dielectric resonator inserted in the center of a cavity [31]. The holder is made of a material with low loss and low permittivity, such as Teflon, so its effect is negligible. The dielectric resonator and the cavity are labeled resonator 1 and resonator 2 respectively. Two types of dielectric resonators are used in this article, namely *types I* and *II*. For *type I* $\varepsilon_r = 29.2$, $d_1 = 6$ mm, $l_1 = 2.65$ mm and $f \approx 9.7$ GHz. In contrast, for *type II* $\varepsilon_r = 261$ and $d_1/l_1 = 1$. The terms d and l are the resonators' diameter and height respectively. The cavity also has an aspect ratio of $d_2/l_2 = 1$.

The two modes of interest are the dielectric $TE_{01\delta}$ mode and the cavity TE_{011} mode. The electric field of each mode can be written as [33],

$$E_{\varphi 1} = M_1 J_1(k_1 r)\begin{cases} \cos(\beta z) & r \leqslant \frac{d_1}{2}, |z| \leqslant \frac{l_1}{2} \\ e^{\frac{\alpha l_1}{2}} \cos\left(\frac{\beta l_1}{2}\right) e^{-\alpha|z|} & r < \frac{d_1}{2}, |z| > \frac{l_1}{2} \end{cases}$$

and

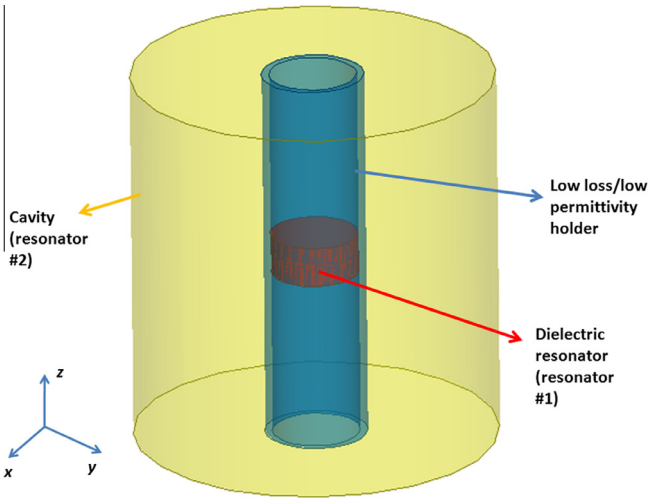

Fig. 1. A probe formed by a dielectric resonator inserted in a conducting cavity. The dielectric insert is held inside a hollow low loss/low permittivity holder.

$$E_{\varphi 2} = M_2 J_1(k_2 r)\cos\left(\frac{\pi z}{l_2}\right). \quad (3)$$

Eq. (2) describes the DR in free space. Usually for small cavities the planar walls are imposed as boundary conditions. However here the effect of the cavity walls is ignored because the DR is fixed in the CV center and the distance between the DR and the CV walls is very large. In these equations k_1, k_2 are the radial wave numbers of the dielectric and cavity respectively. $E_{\phi i}$ is the azimuthal electric field component and $M_{1,2}$ are the amplitude of the fields. The corresponding magnetic field values are obtained from Eqs. (2) and (3) using the Maxwell's equations:

$$\mathbf{H}_{1,2} = -\frac{1}{j\omega_{1,2}} \nabla \times \mathbf{E}_{1,2}.$$

In the above equation, $\mathbf{H}_{1,2}$ are the magnetic field intensities and $\omega_{1,2} = 2\pi f_{1,2}$ are the angular frequencies of the DR and CV respectively. In Eq. (2) the DR fields were assumed to be confined within a perfect magnetic wall tube with a diameter equal to the dielectric diameter [39]. The p_{01} term is the root of the 0th order Bessel function $J_0(x)$. It is equal to 2.405. The radial wave number $k_1 = p_{01}/r_1$ while

$$\beta = \sqrt{\varepsilon_r k_0^2 - \left(\frac{2.405}{r_1}\right)^2},$$

where k_0 is the free space wave number. Finally, $r_1 = d_1/2$ and is the DR radius. The perfect magnetic wall approximation gives a maximum error in frequency of 10% less than the actual value [40].

In CMT the fields are expressed as a linear combination of the uncoupled ones as [31]

$$\mathbf{E} = a_1\mathbf{E}_1 + a_2\mathbf{E}_2 \quad (4)$$

and

$$\mathbf{H} = b_1\mathbf{H}_1 + b_2\mathbf{H}_2. \quad (5)$$

Here $\mathbf{E}$ and $\mathbf{H}$ are the coupled electric and magnetic fields respectively. The coupling coefficient, eigenvalues (ω^2) and the eigenvectors (a_i^{++}, a_i^{+-}) were previously found to be [31]

$$\kappa = \frac{\zeta_{12}}{\sqrt{A_{11}A_{22}}} \quad (6)$$

where

$$\zeta_{12} = \varepsilon_0(\varepsilon_r - 1)\int_{DR} \mathbf{E}_1^* . \mathbf{E}_2 dv$$

is the overlap integral. In general, $A_{ij} = \int_V \varepsilon \mathbf{E}_i^* \cdot \mathbf{E}_j dV$ where ε is the permittivity of the probe which is function of position. In the current article the fields are normalized such that

$$A_{11} = A_{22} \quad (7)$$

$$\omega^2 = \frac{\omega_1^2 + \omega_2^2}{2} \pm \sqrt{\left(\frac{\omega_1^2 - \omega_2^2}{2}\right)^2 + \omega_1^2\omega_2^2\kappa^2}, \quad (8)$$

$$a_2^{++} = \left(\frac{1}{2\kappa}(\gamma^2 - 1) + \sqrt{\frac{1}{4\kappa^2}(\gamma^2 - 1)^2 + \gamma^2}\right)a_1^{++}, \quad (9)$$

for the symmetric mode and

$$a_2^{+-} = \left(\frac{1}{2\kappa}(\gamma^2 - 1) - \sqrt{\frac{1}{4\kappa^2}(\gamma^2 - 1)^2 + \gamma^2}\right)a_1^{+-} \quad (10)$$

for the anti-symmetric mode. Here γ^2 is equal to

$$\gamma^2 = \left(\frac{\omega_1}{\omega_2}\right)^2.$$

The reason why only two symmetric and anti-symmetric modes were considered is best explained by a familiar example. A linear combination of atomic orbitals serves as a good analogy from chemical physics. When two atomic orbitals interact they form two molecular orbitals. One is bonding (symmetric) and the other is anti-bonding (anti-symmetric). The resulting simple molecular orbitals give a very clear picture of the bonding and electron distribution of these molecular orbitals. If one strives for extreme accuracy then all atomic orbitals should be considered, as in the case of a complete configuration interaction calculation. This yields very accurate energies but the resulting natural molecular orbitals contain a huge number of components. As a result a clear simple bonding picture is lost. Generally speaking, if all higher modes are included in the CMT field expansions, the resulting properties would be very accurate but the physical insight of these properties would be too complex to analyze and comprehend.

When the CV and DR modes are degenerate ($\omega_1 = \omega_2 = \omega_0$) the resonance frequency splits into two $\omega^{++} = \omega_0\sqrt{1-\kappa}$ and $\omega^{+-} = \omega_0\sqrt{1+\kappa}$ with corresponding eigenvectors $a_2/a_1 = 1$ and $a_2/a_1 = -1$. When $\omega_1 \gg \omega_2$ or $\omega_1 \ll \omega_2$ and the coupling coefficient is small, the symmetric mode always tends to the lower frequency resonator's mode while the anti-symmetric mode tends to the higher mode.

3. Theoretical derivations, results and discussion

Equipped with Eqs. (6), (8), (9), and (10), expressions for the resonator parameters such as the coupling coefficient κ, the quality factor Q and the filling factor η are derived.

3.1. Coupling coefficient

The coupling coefficient is found using Eq. (6) in conjunction with the fields given in Eqs. (2) and (3). In addition, A_{11} and A_{22} are also required. For the cavity A_{22} can be written as follows [33]

$$A_{22} = \frac{\varepsilon_0 r_2^2 d_2 \pi J_0^2(p'_{01}) M_2^2}{2},$$

where r_2 is the cavity radius, p'_{01} is the first root of $J'_0(x)$ and M is the amplitude of the electric field. Similarly using Eq. (2) A_{11} takes the form

$$A_{11} = \frac{\varepsilon_0 \varepsilon_r r_1^2 \pi J_1^2(k_1 r_1) M_1^2}{2}\left(\frac{\sin\beta l_1}{\beta + l_1}\right).$$

The overlap integral is

$$\zeta_{12} = M_1 M_2 2\pi\varepsilon_0(\varepsilon_r - 1)\frac{p'_{01}}{p_{01}}\frac{r_1^3}{r_2}J_2(k_1 r_1)\frac{1}{\beta}\sin\frac{\beta l_1}{2}.$$

Here the following approximations $J_1(k_c r) \approx \frac{1}{2}k_c r, l_1 \ll l_2$ and $\beta \gg \frac{\pi}{l_2}$ together with the $\frac{d}{dx}x^2 J_2(x) = x^2 J_1(x)$ recurrence relation were used [41]. Consequently, the coupling coefficient given by (6) can be written as,

$$\kappa = 13.16\frac{(\varepsilon_r - 1)}{\sqrt{2\varepsilon_r \beta l_2}}\left(\frac{r_1}{r_2}\right)^2\sqrt{\frac{1-\cos\beta l_1}{\beta l_1 + \sin\beta l_1}}$$

or

$$\kappa = 13.16\frac{(\varepsilon_r - 1)}{\sqrt{2\varepsilon_r \beta l_2}}\frac{S_1}{S_2}\sqrt{\frac{1-\cos\beta l_1}{\beta l_1 + \sin\beta l_1}}. \quad (11)$$

In this case S_1 and S_2 are the dielectric and cavity cross sectional areas respectively. The above equation shows that, as long as the dielectric constant is large, the dependence of the coupling coefficient on ε_r is moderate (of the order of $\sqrt{\varepsilon_r}$) compared to its dependence on the ratio of the two overlap areas S_1/S_2.

The formulae derived in the previous paragraphs are applied to type *I* and type *II* resonators when inserted in a cylindrical cavity. The DR operates in the $TE_{01\delta}$ mode and the cavity resonates in its TE_{011} mode. From Eq. (11), the coupling coefficient is related to the relative permittivity and areas by

$$\kappa \propto \sqrt{\varepsilon_r}\frac{S_1}{S_2}. \quad (12)$$

When the diameter and height of the *type II* DR are in the range of 1.3–2.1 mm,

$$\frac{\kappa_{\varepsilon_r=30}}{\kappa_{\varepsilon_r=261}} \approx 3 \sim 8.$$

A large coupling coefficient will certainly increase the dielectric effect of the probe, which in turn improves the SNR compared to that of an empty cavity. Since multifrequency/multifield magnetic experiments are becoming increasingly important there is a need by researchers for probes consisting of DR and CV that operate at different frequencies. The main restriction is the availability of DR materials with a suitable ε_r to efficiently couple with the CV. However, Relation (12) shows that the coupling can be also controlled by the S_1/S_2 factor. This provides the spectroscopist with an additional degree of freedom.

It is interesting to compare the values of κ, derived here using CMT and those computed using the LCM proposed in Ref. [30]. In analyzing the circuit model, the coupling coefficient, is labeled κ' to distinguish it from the one given by Eq. (11). It is found to be [30]

$$\kappa' = \omega_1\omega_2\sqrt{L_c C_{cc} L_d C_{cc}}, \quad (13)$$

where L_c, L_d are the cavity and dielectric inductance respectively while C_{cc} is the coupling capacitance. Here it was assumed that $C_{cc} \ll C_c, C_d$ and $L_{c,d}C_{cc} \ll (1/\omega_{1,2}^2)$. The exact expressions for these LC parameters have been defined previously [30]. Noting that

$$\omega_1^2 = 1/L_d C_d$$

and

$$\omega_2^2 = 1/L_c C_c$$

Eq. (13) can be written as

$$\kappa' = C_{cc}/\sqrt{C_d C_c}.$$

By using the formulae for C_{cc}, C_d and C_c one gets [30]

$$\kappa' = 2\frac{1}{\sqrt{2\varepsilon_r \beta d_2}}\sqrt{2(\beta l_1 + \sin\beta l_1)}. \quad (14)$$

The coupling coefficient given by Eq. (14) is different from Eq. (11), obtained using CMT. The main difference is the absence of the explicit dependence on the area overlap S_1/S_2. Unlike Eq. (11), provided all other parameters are fixed, Eq. (14) suggests that κ' is inversely proportional to $\sqrt{\varepsilon_r}$.

The discrepancies between Eqs. (11) and (14) do not have a drastic effect particularly when the DR and CV modes are nearly degenerate. To clarify this point, a type *II* DR is inserted in a cavity ($d_2 = l_2 = 4.1598$ cm, $f_{TE_{011}} = 9.5$ GHz) and the coupling coefficients κ and κ' are calculated. In these two equations, the β parameter is the wave number along the dielectric material axis. It can be determined by solving the transcendental equation [33,39]

$$\tan\left(\frac{\beta l_1}{2}\right) = \frac{\alpha}{\beta}.$$

Here α is the decay constant in free space and it is equal to $\alpha = \sqrt{(2.405/r_1)^2 - k_0^2}$. The calculated κ and κ' are plotted versus the diameter of the DR over the interval ($d_1 = l_1 = 1.3 - 2.1$ mm).

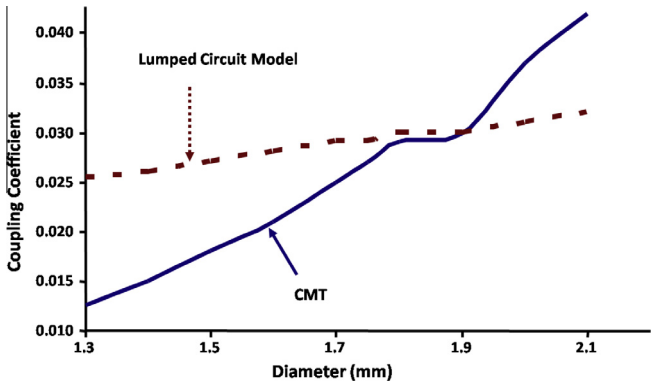

Fig. 2. Coupling coefficient using CMT and the LCM. The cavity has a fixed dimension of $d_2 = l_2 = 4.1598$ cm and the dielectric resonator has a high relative permittivity of 261 and its dimension was allowed to change, where $d_1 = l_1$.

The results are depicted in Fig. 2. All calculations were performed using Maple 13™ suite of programs (MapleSoft, a subsidiary of Cybernet Systems Co. Ltd.).When designing EPR probes the frequencies of the DR and CV are chosen to be nearly degenerate. In this situation, ($l_1 \approx 1.75 - 1.95$ mm), it is clear from Fig. 2 that the discrepancy between κ and κ' calculated using both methods is small. Consequently the magnetic resonance spectroscopists have available two independent and complimentary methods to assess their probes.

To check the percentage errors of both CMT and LCM, the symmetric and anti-symmetric frequencies are also calculated. The deviations, compared to ANSOFT HFSS® (Ansys Corporation, Pittsburgh, PA, USA) simulations, are shown in Fig. 3. The HFSS program uses finite element methods to numerically solve for the electromagnetic fields and frequencies subjected to the boundary conditions. The relative frequency tolerance was taken to be less than 0.1%.

In Fig. 3 the CMT percentage errors relative to the reference finite element simulations are smaller when compared to those of the LCM. This is particularly clear when the frequencies of the two uncoupled modes are not close to one another. Since the coupled frequencies depend on κ and κ', therefore Figs. 2 and 3 indicate that CMT method gives more accurate coupling coefficient values. In addition, Fig. 2 shows that the coupling coefficient calculated using CMT spans a larger range (0.012–0.04) compared to that computed by the LC method (0.025–0.03).

Previously, the coupled frequencies were calculated using CMT and the LCM for a configuration of a *type I* resonator in a cavity where the cavity's diameter was allowed to change from 2.5 cm to 5.4 cm [31]. It was also shown that CMT gives better error curves. As a further logical step, one studies in the current article the behavior of the coupling coefficients given by Eqs. (11) and (14). Hence for this configuration, κ and κ' are calculated and plotted in Fig. 4.

Fig. 4 illustrates that the coupling coefficient for type *I* resonators is an order of magnitude higher than that shown in Fig. 2. This is attributed to the increase in the overlap area S_1/S_2. Again, the calculated κ and κ' using both methods, are close when the resonators are nearly degenerate. Consequently, one can conclude that the LCM can predict the system's behavior especially when the two resonators are degenerate. For EPR probes, when the CV acts as a shield with a small diameter, Fig. 4 shows that κ is large (0.25–0.45). This is quite significant and should be taken into account when designing an EPR probe.

The degree of coupling is defined by the ratio $|a_2/a_1|$. This parameter determines the CV component relative to the DR component. The larger the parameter value, the higher the CV mode portion in the coupled mode. From Eqs. (9) and (10), it takes the forms

$$\left(\frac{1}{2\kappa}(\gamma^2-1)+\sqrt{\frac{1}{4\kappa^2}(\gamma^2-1)^2+\gamma^2}\right)$$

and

$$\left(\frac{1}{2\kappa}(\gamma^2-1)-\sqrt{\frac{1}{4\kappa^2}(\gamma^2-1)^2+\gamma^2}\right)$$

for the symmetric and anti-symmetric mode respectively. Fig. 5 illustrates the behavior of $|a_2/a_1|$ with respect to $\gamma^2 = (\omega_1/\omega_2)^2$ for different coupling coefficient values.

Fig. 5 shows that when κ increases $|a_2/a_1|$ decreases. From the comparable values of a_1 and a_2 of Eq. (4) it is seen that the modes tend to stay coupled. This is best observed in the anti-symmetric mode when $\gamma^2 < 1$. It corroborates the previous observations that, under these conditions, the anti-symmetric mode slowly decouples for *type I* resonators [31].

3.2. Filling factor

The filling factor, η, is a measure of the concentration of the magnetic field at the sample and is equal to [38]

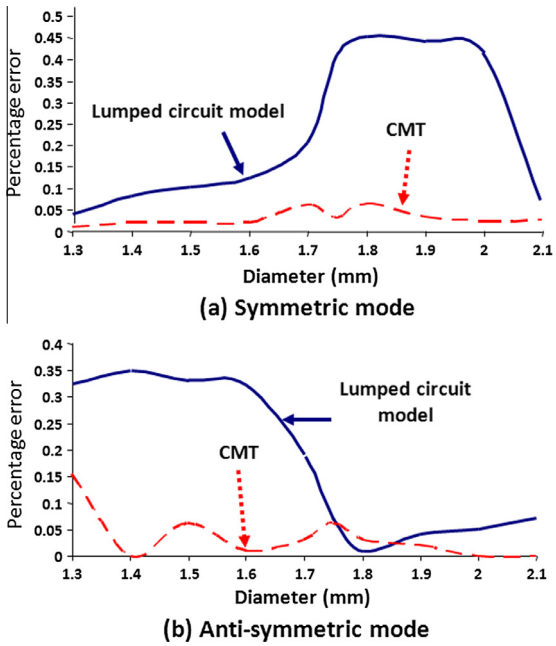

Fig. 3. The percentage error of the coupled modes frequencies using the CMT and LCM. The DR diameter and height are equal and changes from 1.3 to 2.1 mm.

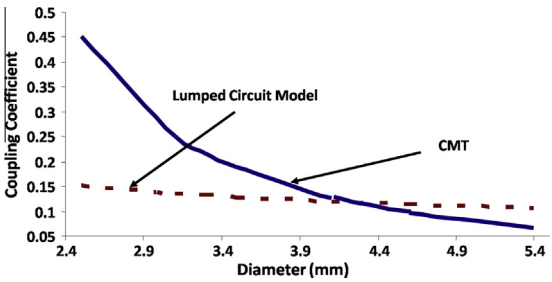

Fig. 4. Coupling coefficient for type *I* resonator inserted in a CV. The CV's diameter was allowed to change from 2.5 to 5.4 cm. Here $d_2 = l_2$.

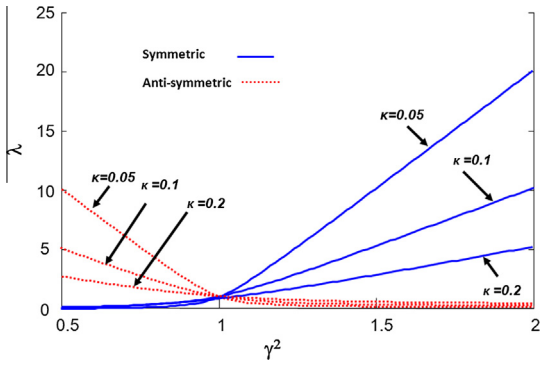

Fig. 5. The ratio $|a_2/a_1| \equiv \lambda$ plotted versus the ratio $\gamma^2 = (\omega_1/\omega_2)^2$ for different κ values. Small $|a_2/a_1|$ values signify a large DR component.

$$\eta = \frac{\int_{Vsample} |\mathbf{H}_\perp|^2 dV}{\int_{CV} |\mathbf{H}|^2 dV}.$$

Here $|\mathbf{H}_\perp|$ is the magnetic field intensity perpendicular to the static magnetic field. To calculate the filling factor, η, of the coupled system, one takes the complex conjugate of the magnetic field of Eq. (5), and integrates over the sample and total volumes. Thus η is found, after using the normalization condition (7), to be

$$\eta = |a_1|^2\eta_1 + |a_2|^2\eta_2 + 2a_1a_2 \int_{Vsample} \mu_0 \mathbf{H}_1 \cdot \mathbf{H}_2 dv.$$

When the overlap is negligible, this equation reduces to

$$\eta \approx |a_1|^2\eta_1 + |a_2|^2\eta_2.$$

When the frequencies ω_1 and ω_2 differ significantly the filling factor of the coupled system can be determined by referring to Fig. 5. For example for the symmetric mode, when $\omega_1 \gg \omega_2$, $|a_2/a_1|$ is large. In this case, the filling factor approaches the CV value.

For the degenerate case the magnitude of the expansion coefficients of both the symmetric and anti-symmetric modes in Eq. (4) are equal to $1/\sqrt{2}$. Thus the filling factor of the modes is the average of the DR and CV filling factors,

$$\eta = \frac{1}{2}(\eta_1 + \eta_2). \tag{15}$$

This is a direct consequence of the fact that when the two uncoupled modes have equal frequencies, the resulting coupled modes have equal contributions from the uncoupled modes. For a DR with a high filling factor $\eta_1 \gg \eta_2$ Eq. (15) is approximately

$$\eta = \frac{1}{2}\eta_1. \tag{16}$$

Therefore, Eq. (16) implies that by inserting a DR in a CV, the filling factor is automatically cut in half. This is a direct consequence of the equal components of $\mathbf{H}_1$ and $\mathbf{H}_2$ when their frequencies are degenerate [31]. This important result in conjunction with Q is vital for EPR spectroscopist concerned with signal intensities where estimating the number of spins is important.

3.3. Quality factor

The quality factor, Q, is an important parameter in EPR spectroscopy because it affects the probe's signal intensity. As was previously mentioned in the introduction, the overall Q of the coupled system together with κ determine whether or not the coupled modes overlap. Therefore in this article, an expression for Q is derived. The quality factor of a resonator is defined as [33]

$$Q = \frac{2\omega W_E}{P_l}, \tag{17}$$

where ω is the angular frequency of the coupled modes, W_E is the average stored electrical energy (at resonance, it is also equal to the average stored magnetic energy) and P_l is the average power loss. Expressing the energy in terms of the eigenvectors one arrives at

$$W_E = \frac{1}{4}\int_V \varepsilon(a_1\mathbf{E}_1 + a_2\mathbf{E}_2) * (a_1\mathbf{E}_1 + a_2\mathbf{E}_2) dV$$
$$= \frac{1}{4}\sum_{i=1}^{2}\sum_{j=1}^{2} a_i^* A_{ij} a_j. \tag{18}$$

Similarly the power loss, P_l, is the sum of the losses inside the dielectric material, P_{ld}, and the loss on the conductor walls, P_{lc}.

$$P_l = P_{ld} + P_{lc}. \tag{19}$$

They are equal to

$$P_{ld} = \frac{\sigma}{2}\int_{DR} |\mathbf{E}|^2 dV, \tag{20}$$

and

$$P_{lc} = \frac{R_s}{2}\int_{Cavity} |\mathbf{H}_{\tan}|^2 dS. \tag{21}$$

Here σ is the dielectric conductivity and R_s is the cavity surface resistance.

Using expansions (4) and (5), the energy and power values given by Eqs. (18)–(21), can be re-written as

$$W_E = \frac{\sum_{ij} a_i^* a_j \int_V \varepsilon \mathbf{E}_i^* \cdot \mathbf{E}_j dv}{4}, \tag{22}$$

$$P_{ld} = \sum_{i,j} a_i^* a_j \frac{\sigma}{2}\int_{DR} \mathbf{E}_i^* \cdot \mathbf{E}_j dV, \tag{23}$$

and

$$P_{lc} = \frac{R_s}{2}\sum_{i,j} b_i^* b_j \int_{\partial V} \mathbf{H}_i^* \cdot \mathbf{H}_j dS. \tag{24}$$

When the coupling is small the overlap area S_1/S_2 is also small and the above relations can be approximated as

$$W_E \approx \frac{a_1^2\int_V \varepsilon|\mathbf{E}_1|^2 dv + a_2^2\int_V \varepsilon|\mathbf{E}_2|^2 dv}{4} = \frac{a_1^2 A_{11} + a_2^2 A_{22}}{4},$$

$$P_{ld} \approx |a_1|^2 P_{ld}^{DR}$$

and

$$P_{lc} \approx |b_2|^2 P_{lc}^{CV}.$$

Here P_{ld}^{DR} and P_{lc}^{CV} are the power losses for the dielectric insert and cavity respectively. Using the normalization condition (7), one can express the quality factor, given by (17), for the coupled system as

$$\frac{\omega}{Q} = \frac{|a_1|^2\omega_1}{Q_1} + \frac{|b_2|^2\omega_2}{Q_2}. \tag{25}$$

Here

$$Q_1 = \frac{\omega_1}{2P_{ld}^{DR}} \tag{26}$$

and

$$Q_2 = \frac{\omega_2}{2P_{lc}^{CV}}. \tag{27}$$

They are the quality factors of the dielectric and cavity resonators respectively. The power loss due to the iris, P_{iris}, can be taken into

account by noting that it occurs at the iris cavity interface and is mainly due to the CV fields. Thus Q_2 is taken to be the quality factor of the loaded CV. Taking into account that $a_i \approx b_i$, the total loss is [31]

$$P_l = \frac{1}{2}\left(\frac{\omega_1|a_1|^2}{Q_1} + \frac{\omega_2|a_2|^2}{Q_2}\right). \tag{28}$$

From Eqs. (25)–(28) one comes to the important conclusion that the overall Q factor of the coupled modes is a function of the individual Qs of its resonant components. This is a different picture that emerges directly from the CMT treatment. Normally for an EPR spectrometer, one chooses a DR and a CV with approximately the same resonance frequency to maximize their interaction. Specifically for the degenerate case, $\omega_1 = \omega_2 = \omega_0$ and $|a_1| = |a_2| = |b_1| = |b_2| = 1/\sqrt{2}$, The quality factors of the coupled modes become

$$Q^{++} = 2\sqrt{1-|\kappa|}\frac{Q_1Q_2}{Q_1+Q_2}, \tag{29}$$

and

$$Q^{+-} = 2\sqrt{1+|\kappa|}\frac{Q_1Q_2}{Q_1+Q_2}. \tag{30}$$

where Q^{++} and Q^{+-} are the Q factors for the symmetric and anti-symmetric modes respectively. From Eqs. (29) and (30) it is clear that the two values are slightly different. The difference between them is

$$Q^{+-} - Q^{++} \approx 2|\kappa|\frac{Q_1Q_2}{Q_1+Q_2}.$$

For a small κ, the coupled Q reduces to

$$Q = Q^{++} \approx Q^{+-} \approx 2\frac{Q_1Q_2}{Q_1+Q_2}. \tag{31}$$

Towards the end of this section, the CV and DR modes are degenerate where it is assumed that $Q^{++} = Q^{+-}$ and are given by Eq. (31).

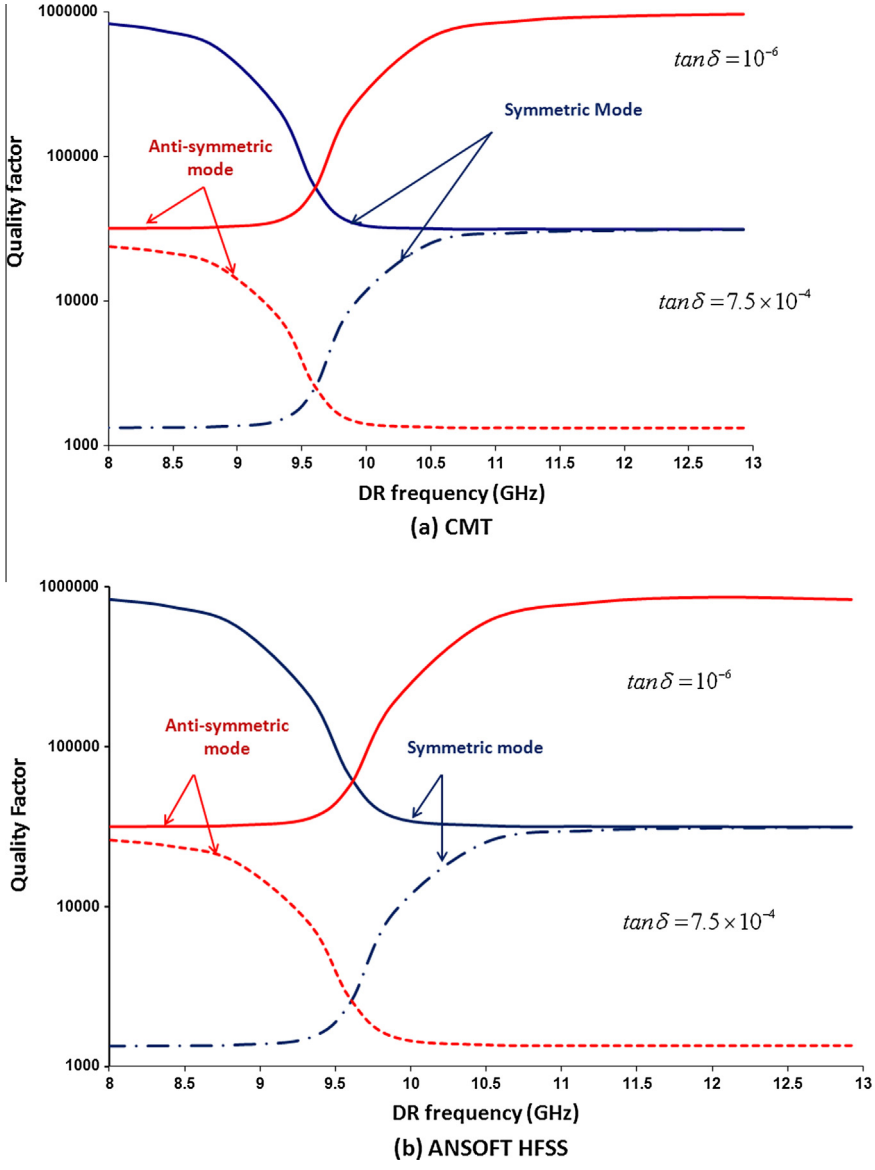

Fig. 6. The quality factor for an EPR probe consisting of a *type II* resonator inserted in a silver-plated cavity. The resonators' dimensions were allowed to change from $d_1 = l_1 = 1.3 - 2.1$ mm resulting in a frequency change from 8.0 to 13.0 GHz. (a) Using CMT. (b) Using HFSS. To accommodate the wide range of the Q values the y axis is drawn on a logarithmic scale.

When there is a large difference between Q_1 and Q_2, Eq. (31) predicts that

$$Q \approx 2\min(Q_1, Q_2). \tag{32}$$

Two limiting situations are of interest. The first is when $Q_1 \ll Q_2$. It arises when the DR is lossy or houses a lossy sample. In this case and according to Eq. (16), although the high dielectric constant increases the filling factor of the probe, it is at the expense of lowering the overall Q. This can be understood by referring to Eq. (1). For unsaturated samples and provided that the power is kept constant, the ratio of signal intensity of the coupled structure to that of an empty cavity is

$$\frac{I_{with\ insert}}{I_{empty}} = \frac{\eta_{with\ insert}}{\eta_{empty}} \times \frac{Q_{with\ insert}}{Q_{empty}}. \tag{33}$$

The signal intensity $I_{with\ insert}$ is calculated at the frequencies of the coupled modes while I_{empty} is calculated at the CV frequency ω_2. In this situation and using Eqs. (32) and (16), the above expression simplifies to

$$\frac{I_{with\ insert}}{I_{empty}} = \frac{\eta_1}{\eta_2} \times \frac{Q_1}{Q_2}. \tag{34}$$

Thus the change in signal intensity due to the insertion of the DR is dependent on the quality and filling factors of both resonant structures. Thus when designing experiments one must take into consideration the effect of Q_1 and Q_2 in addition to the filling factors of the resonating components. It is worth mentioning that a low Q is desirable in pulsed EPR spectroscopy shortens the probe's dead time which enables faster averaging.

The second situation is when $Q_1 \gg Q_2$ for example, when the DR is made of sapphire or a ceramic material. At constant power, using Eq. (16) and noticing that $Q \approx 2Q_{min} = 2Q_2$, the ratio of signal intensity of the coupled structure to that of an empty CV is,

$$\frac{I_{with\ insert}}{I_{empty}} = \frac{\eta_1}{2} \cdot \frac{1}{\eta_2} \cdot \frac{2Q_2}{Q_2} = \frac{\eta_1}{\eta_2}. \tag{35}$$

In this case $I_{with\ insert}/I_{empty}$ depends only on the ratio of the filling factors. This is the optimal upper bound of signal enhancement.

For any Q value, $I_{with\ insert}/I_{empty}$ is obtained from Eqs. (31) and (16), to give

$$\frac{I_{with\ insert}}{I_{cavity}} \approx \left(\frac{\eta_1}{\eta_2}\right) \cdot \left(\frac{Q_1}{Q_1 + Q_2}\right). \tag{36}$$

This general expression tends to Eqs. (34) and (35) when $Q_1 \ll Q_2$ and $Q_1 \gg Q_2$ respectively. From a practical point of view, when designing a probe one needs to maximize $I_{with\ insert}/I_{empty}$. This may be obtained by selecting a DR such that $Q_1 \gg Q_2$ rendering the last term in the right hand side of Eq. (36) effectively unity. For example a TE_{102} cavity with $Q_2 \sim 3000$ and $\nu_2 = 9.5$ GHz can be enhanced using a ceramic resonator (muRata F series, DRT type) with a $Q_1 \sim 35{,}000$ and $\nu_1 = 9.5$ GHz. The coupling coefficient is estimated to be $\approx 0.1 - 0.3$ and the symmetric and anti-symmetric modes frequencies to be ≈9.2 and 10 GHz respectively.

The expression of the quality factor given by Eq. (25), is applied to three probe cases. The first is a probe made of a high ε_r (high η) *type II* DR inserted in low loss (high Q) cylindrical CV. The CV dimensions are $d_2 = l_2 = 4.1598$ cm and its frequency is $f_{TE_{011}} = 9.5$ GHz. It is silver plated and hence its $Q_2 \approx 32{,}000$ and the dielectric material has a loss tangent of 7.5×10^{-4} ($Q_1 = 1333.3$) [30]. The second case is identical to the first in all aspects except that the DR loss tangent is 10^{-6} ($Q_1 = 10^6$). The Q values for the two cases, calculated using CMT, are then compared to those obtained using HFSS® finite elements simulator as shown in Fig. 6a and b.

The figures show an excellent agreement between the CMT Q obtained using Eq. (25) and that by HFSS simulation. In accordance with Eqs. (29) and (30), when the two uncoupled modes are degenerate at ≈ 9.5 GHz, the Q of the coupled structure is approximately double the minimum Q. In particular, it is equal to $2Q_1$ (2600) when the DR has a loss tangent of 7.5×10^{-4} and equal to $2Q_2$ (60,000) for the other configuration (DR loss tangent = 10^{-6}).

The third case involves a *type I* DR with a moderate ε_r of 29.2. In this case κ is high and the overlap terms which were neglected in the derivation of expression (25) are no longer small. This would be even more prominent when the DR has an even lower permittivity such as sapphire. Therefore, one needs to apply the general expressions for the stored energy and power losses (22)–(24). These general expressions still apply and give very accurate values for the quality factors. For this configuration the cavity dimensions are allowed to change from 3.4 cm to 5.4 cm. This corresponds to a span

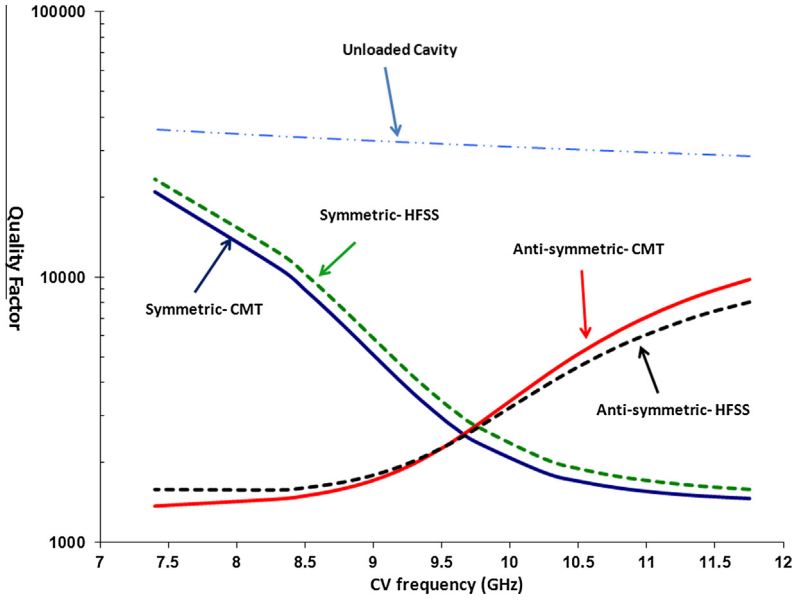

Fig. 7. The quality factor for *type I* resonator. The cavity diameter is allowed to change from $d_2 = l_2 = 3.4$ cm to $d_2 = l_2 = 5.4$ cm. The corresponding CV frequency ranges from 7.5 to 11.7 GHz and dielectric loss tangent is 7.5×10^{-4}.

of ±2 GHz around the uncoupled degenerate frequency ($f \approx 9.7$ GHz). The results are compared to HFSS® simulations, as shown in Fig. 7.

In contrast to Fig. 6a and b where the quality factors approach those of the uncoupled structures at the extreme right and left, Fig. 7 shows that the system is still coupled in the range of 3.4–5.4 cm. From Fig. 7, over a 4 GHz range the quality factor of the symmetric mode varies from 1300 to 20,000 while that of the anti-symmetric one goes only from 1300 to 10,000. This indicates that the symmetric mode decouples more readily than the anti-symmetric one. This corroborates the previous findings in Fig. 5 of Ref. [31].

Finally, in practical situations one needs to excite only one of the coupled modes (either the symmetric or anti-symmetric). There are three conditions to be fulfilled to efficiently excite a particular mode [30]. The field emanating from the exciting iris should be collinear with the field of the mode. This depends on the geometry of the iris which is beyond the scope of this paper. The field of the mode should have enough strength at the vicinity of the iris. Obviously this is large when the coupled mode has a significant CV component and B_1 at the sample. Lastly, the driving source's frequency should be within $\pm 5BW = \pm 5(f/Q)$ of the mode's frequency. Therefore, it is vital to calculate how well the two modes are separated. One way is to find the ratio of the difference between the two coupled frequencies versus the average bandwidth or

$$\Phi = \frac{f_{anti} - f_{sym}}{0.5(BW_{sym} + BW_{anti})}.$$

The minimum separation distance between the coupled modes occurs at the avoided crossing when the two modes are degenerate. Noting that $BW = f/Q$, and Eqs. (29) and (30), one can find that Φ

$$\Phi = 2\kappa \frac{Q_1 Q_2}{Q_1 + Q_2}.$$

For *type II* ferroelectric resonators when the dielectric loss tangent is 7.5×10^{-4}, Φ is found to be ≈62. For type *I* resonators with the same loss tangent, Φ is approximately 375. Therefore, the frequencies of the two modes are well separated for both types of resonators.

The case where the modes may overlap will only occur when the permittivity is very high, the quality factor is low and the coupling coefficient decreases according to Eq. (11). This is because for the same frequency a DR with a high ε_r must have a smaller S_1 compared to one with a lower ε_r. From the relation given by (12), the net result is a decrease in κ.

4. Summary and conclusions

Using CMT, expressions for κ, Q, and η of a probe consisting of a cavity with a dielectric insert are obtained. The κ is found to be proportional to the square root of the relative permittivity as well as to the overlap area. It is CMT values are compared to those derived using the LCM in Ref. [30]. It is found that both methods are in agreement when the uncoupled modes are degenerate. However CMT κ spans a larger range of values. The errors calculated using both methods show that although both the LCM and CMT give excellent results, the CMT is more accurate. The coupling coefficient of a cavity with a DR ($\varepsilon_r \approx 30$) is an order of magnitude larger than that of a DR with a very high relative permittivity ($\varepsilon_r \approx 261$). This is due to the increase in the overlap area, S_1/S_2. This also explains why, in the case of a shield ($\omega_2 \gg \omega_1$), the anti-symmetric mode has a significant dielectric component. Therefore, the dielectric can be used to improve the cavity signal intensity.

A simple expression for η of the coupled system is derived. When the resonators are degenerate, it is shown that coupled η is the average of the two uncoupled ones. Moreover when designing EPR probes, the CV filling factor is small and can be ignored. In this situation, the coupled η is approximately half of that of the DR.

A closed form expression for Q of the coupled system was derived. It was shown that the quality factor depends on the eigenvectors, uncoupled frequencies (ω_1, ω_2) and the uncoupled quality factors (Q_1, Q_2). The expression is applied to the DR with a high dielectric constant ($\varepsilon_r \approx 261$) but with different loss tangents ($\tan\delta = 7.5 \times 10^{-4}$ and $\tan\delta = 10^{-6}$). The resulting values are found to agree with the corresponding HFSS® simulations quite well. Compared to that of the empty cavity and when the Q of the DR is much smaller than that of the cavity, the coupled quality factors decrease significantly. This affects the signal intensity. In general when the resonators are degenerate, Q is approximately equal to double the minimum of Q_1 and Q_2 provided there is a large difference between the two.

For relatively moderate dielectric inserts ($\varepsilon_r \approx 30$), κ is large. Therefore, the overlap integral must be considered when calculating the quality factors. Taking this into account CMT is still capable of calculating the quality factors especially near the degenerate condition.

Based on the expressions derived for the quality and filling factors, the signal enhancement ratio, $I_{with\ insert}/I_{empty}$, is also derived. For low loss DRs $I_{with\ insert}/I_{empty}$ is only dictated by η_1/η_2 and is independent of the quality factors. However, when the DR insert has a low Q, both the uncoupled Qs and η s are needed to determine the signal enhancement.

The separation between the modes, Φ, is calculated for the two types of DRs in terms of κ and Q. The separation between the frequencies of the two coupled modes is significantly greater than five times the average bandwidth. Consequently, exciting one coupled mode will probably not excite the other one. However, if ε_r increases κ decreases and Q of the DR insert is not large enough, then the two modes may overlap.

The expressions derived in this article are quite general. Thus they can be applied to the case of a loop-gap inserted in a cavity. However, coupling with other CV modes may occur. This article suggests that for effective EPR probe design, one needs to evaluate the different parameters, κ, η, Q and Φ. For example, a DR insert with a low Q may negatively affect the signal intensity. Moreover for extremely high DR loss tangents and/or for lossy samples, the coupled modes may overlap. Therefore optimization of the above parameters, using the equations derived here, is needed for the design of an efficient EPR probe.

Acknowledgments

SMM acknowledges the Natural Sciences and Engineering Research Council of Canada for financial support in the form of a discovery (operating) grant. SYN is grateful for the financial assistance from the University of New Brunswick and the Department of Electrical and Computer Engineering in the form of pre-doctoral teaching and research assistantships. We would like to acknowledge CMC Microsystems for providing the HFSS suite of programs that facilitated this research.

References

[1] M. Bennati, T.F. Prisner, New developments in high field electron paramagnetic resonance with applications in structural biology, Rep. Prog. Phys. 68 (2005) 411–448.
[2] A. Schweiger, G. Jeschke, Principles of Pulsed Electron Paramagnetic Resonance, Oxford University Press, Oxford, 2001.
[3] G.R. Eaton, S.S. Eaton, Electron-nuclear double resonance spectroscopy and electron spin echo envelope modulation spectroscopy, Compr. Coord. Chem. II (2) (2004) 49–55.
[4] M.M. Hertel, V.P. Denysenkov, M. Bennati, T.F. Prisner, Pulsed 180-GHz EPR/ENDOR/PELDOR spectroscopy, Magn. Reson. Chem. 43 (2005) S248–S255.

[5] L.D. Kispert, Electron-electron double resonance, Biol. Magn. Reson. 24 (2005) 165–197.
[6] Y.D. Tsvetkov, Peptide aggregation and conformation properties as studied by pulsed electron-electron double resonance: pulsed ELDOR in spin labeled peptides, Biol. Magn. Reson. 21 (2004) 385–433.
[7] S.S. Eaton, G.R. Eaton, Measurements of interspin distances by EPR, Electron Paramagn. Reson. 19 (2004) 318–337.
[8] J. McCracken, Electron spin echo envelope modulation (ESEEM) spectroscopy, Appl. Phys. Methods Inorg. Bioinorg. Chem. (2007) 55–77.
[9] P.P. Borbat, J.H. Davis, S.E. Butcher, J.H. Freed, Measurement of large distances in biomolecules using double-quantum filtered refocused electron spin-echoes, J. Am. Chem. Soc. 126 (2004) 7746–7747.
[10] Y.W. Chiang, P.P. Borbat, J.H. Freed, The determination of pair distance distributions by pulsed ESR using Tikhonov regularization, J. Magn. Reson. 172 (2005) 279–295.
[11] S.K. Misra, P.P. Borbat, J.H. Freed, Calculation of double-quantum-coherence two-dimensional spectra: distance measurements and orientational correlations, Appl. Magn. Reson. 36 (2009) 237–258.
[12] J.E. Banham, C.M. Baker, S. Ceola, I.J. Day, G.H. Grant, E.J.J. Groenen, C.T. Rodgers, G. Jeschke, C.R. Timmel, Distance measurements in the borderline region of applicability of CW EPR and DEER: a model study on a homologous series of spin-labeled peptides, J. Magn. Reson. 191 (2008) 202–218 (1969–1992).
[13] P.G. Fajer, Site directed spin labelling and pulsed dipolar electron paramagnetic resonance (double electron-electron resonance) of force activation in muscle, J. Phys. Condens. Matter 17 (2005) S1459–S1469.
[14] L. Millhauser Glenn, Copper and the prion protein: methods, structures, function, and disease, Annu. Rev. Phys. Chem. 58 (2007) 299–320.
[15] R.W. Dykstra, G.D. Markham, A dielectric sample resonator design for enhanced sensitivity of EPR spectroscopy, J. Magn. Reson. 69 (1986) 350–355.
[16] W. Froncisz, J.S. Hyde, The loop-gap resonator: a new microwave lumped circuit ESR sample structure, J. Magn. Reson. 47 (1982) 515–521.
[17] J.P. Hornak, J.H. Freed, Electron spin echoes with a loop-gap resonator, J. Magn. Reson. 62 (1985) 311–313.
[18] A. Blank, E. Stavitski, H. Levanon, F. Gubaydullin, Transparent miniature dielectric resonator for electron paramagnetic resonance experiments, Rev. Sci. Instrum. 74 (2003) 2853–2859.
[19] I. Golovina, I. Geifman, A. Belous, New ceramic EPR resonators with high dielectric permittivity, J. Magn. Reson. 195 (2008) 52–59.
[20] M. Jaworski, A. Sienkiewicz, C.P. Scholes, Double-stacked dielectric resonator for sensitive EPR measurements, J. Magn. Reson. 124 (1997) 87–96 (1969–1992).
[21] S.M. Mattar, A.H. Emwas, A tuneable doubly stacked dielectric resonator housed in an intact TE102 cavity for electron paramagnetic resonance spectroscopy, Chem. Phys. Lett. 368 (2003) 724–731.
[22] Y.E. Nesmelov, J.T. Surek, D.D. Thomas, Enhanced EPR sensitivity from a ferroelectric cavity insert, J. Magn. Reson. 153 (2001) 7–14.
[23] A. Raitsimring, A. Astashkin, J.H. Enemark, A. Blank, Y. Twig, Y. Song, T.J. Meade, Dielectric resonator for Ka-band pulsed EPR measurements at cryogenic temperatures: probehead construction and applications, Appl. Magn. Reson. 42 (2012) 441–452.
[24] F.J. Rosenbaum, Dielectric cavity resonator for ESR experiments, Rev. Sci. Instrum. 35 (1964) 1550–1554.
[25] A. Sienkiewicz, K. Qu, Dielectric resonator-based stopped-flow electron paramagnetic resonance, Rev. Sci. Instrum. 65 (1994) 68–74.
[26] S. Pfenninger, J. Forrer, A. Schweiger, T. Weiland, Bridged loop–gap resonator: a resonant structure for pulsed ESR transparent to high-frequency radiation, Rev. Sci. Instrum. 59 (1988) 752–760.
[27] K. Qu, J.L. Vaughn, A. Sienkiewicz, C.P. Scholes, J.S. Fetrow, Kinetics and motional dynamics of spin-labeled yeast iso-1-cytochrome c: 1. Stopped-flow electron paramagnetic resonance as a probe for protein folding/unfolding of the C-terminal helix spin-labeled at cysteine 102, Biochemistry 36 (1997) 2884–2897.
[28] J.R. Anderson, R.A. Venters, M.K. Bowman, A.E. True, B.M. Hoffman, ESR and ENDOR applications of loop-gap resonators with distributed circuit coupling, J. Magn. Reson. 65 (1985) (1969) 165–168.
[29] S.M. Mattar, S.Y. Elnaggar, Analysis of two stacked cylindrical dielectric resonators in a TE102 microwave cavity for magnetic resonance spectroscopy, J. Magn. Reson. 209 (2011) 174–182 (San Diego, Calif.: 1997).
[30] R.R. Mett, J.W. Sidabras, I.S. Golovina, J.S. Hyde, Dielectric microwave resonators in TE011 cavities for electron paramagnetic resonance spectroscopy, Rev. Sci. Instrum. 79 (2008) 94702.
[31] S.Y. Elnaggar, R. Tervo, S.M. Mattar, Coupling modes, frequencies and fields of a dielectric resonator and a cavity using coupled mode theory, J. Magn. Reson. 238 (2014) 1–7.
[32] J.S. Colton, L.R. Wienkes, Resonant microwave cavity for 8.5–12 GHz optically detected electron spin resonance with simultaneous nuclear magnetic resonance, Rev. Sci. Instrum. 80 (2009). 035106–035106.
[33] D.M. Pozar, Microwave Engineering, second ed., John Wiley and Sons, Hoboken, 2005.
[34] G.R. Eaton, S.S. Eaton, D.P. Barr, R.T. Weber, Quantitative EPR, Springer Wien New York, Germany, 2010.
[35] G.A. Rinard, S.S. Eaton, G.R. Eaton, C.P. Poole Jr., H.A. Farach, Sensitivity in ESR Measurements, Handbook Electron Spin Reson., 1999.
[36] G.A. Rinard, R.W. Quine, S.S. Eaton, G.R. Eaton, Frequency dependence of EPR sensitivity, Biol. Magn. Reson. 21 (2004) 115–154.
[37] G. Feher, Sensitivity considerations in microwave paramagnetic resonance absorption techniques, Bell Sys. Tech. J (1957) 449–484.
[38] J.S. Hyde, W. Froncisz, T. Oles, Multipurpose loop-gap resonator, J. Magn. Reson. 82 (1989) (1969) 223–230.
[39] S.B. Cohn, Microwave bandpass filters containing high-Q dielectric resonators, Microwave Theory and Technique 16 (1968) 218–227.
[40] T. Itoh, R.S. Rudokas, New method for computing the resonant frequencies of dielectric resonators (Short Papers), IEEE Trans. Microwave Theory Tech. 25 (1977) 52–54.
[41] B.W. Lennart Rade, Vector Identity Mathematics Handbook for Science and Engineering, fifth ed., Springer, Lund, Sweden, 2004.